

BULETINUL INSTITUTULUI POLITEHNIC DIN IAȘI

Publicat de UNIVERSITATEA TEHNICĂ "GH. ASACHI", IAȘI

Tomul XLV (XLIX)

Fasc. 3 — 4

Secția

CONSTRUCȚII DE MAȘINI

EXTRAS

COMPARATIVE ANALYSIS OF THE ACTUAL
COMPUTING METHODS OF THE FILM-COOLING
FLAME TUBE TEMPERATURE AT THE
GAS TURBINE MOTORS

BY

VLAD-MARIO HOMUTESCU

1999

Publicat de
Universitatea Tehnică "Gh. Asachi", Iași
Tomul XLV (XLIX), Fasc. 3-4, 1999

Secția

CONSTRUCȚII DE MAȘINI

D.C. 621 438; 536.1

COMPARATIVE ANALYSIS OF THE ACTUAL COMPUTING METHODS OF THE FILM-COOLING FLAME TUBE TEMPERATURE AT GAS TURBINE MOTORS

BY

VLAD-MARIO HOMUTESCU

Abstract. We analyze comparatively the NSM and the LM methods used to calculate the temperature field along a film-cooling flame tube section. For identical conditions are presented the temperature fields calculated with the two methods.

Key words: gas turbine motor, cooling flame tube temperature.

1. Introduction

A large part of the turboengines used nowadays employ the film cooling for the flame tube.

The calculation of the temperature field along the flame tube is necessary for the designing of a new combustion chamber (when serves especially to establish its geometry) and when adapting an existing chamber to the use of another fuel (situation known when adapting airplane engines went out of flight for ground purposes).

There are two methods better known: N a r e j n i i - S u d a r e v [2], [3] and L e f e b v r e [1]. Both methods consider that the working condition of the combustion chamber is a steady one and that the parameter values on the circumference are constant. As a consequence, the temperature of the fire tube in a section perpendicular on the axis is constant.

The paper analyzes comparatively these methods, showing that they give similar results when computing the temperature field along a film-cooling flame tube section.

2. Physico-Mathematical Models

The heat flows in which the flame tube is involved are presented in Fig. 1. Here: R_1 – heat flow exchanged by radiation from the flame to the inner surface of the flame tube; R_2 – heat flow exchanged by radiation from the flame tube to the outer cover of the combustion chamber; C_1 – heat flow exchanged by convection from the flame tube to the cooling air film; C_2 – heat flow exchanged by convection from the outer surface of the flame tube to the secondary air; K – longitudinal conduction heat flow through the flame tube's wall and K_{12} – transversal conduction heat flow through the flame tube's wall.

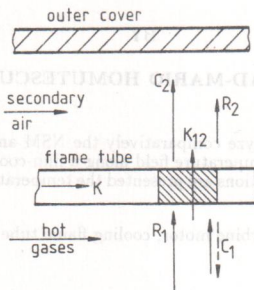


Fig. 1 — Heat flows in which the flame tube is involved.

For a certain part of the flame tube the following relation exists:

$$(1) \quad R_1 + C_1 = R_2 + C_2 = K_{12}.$$

2.1. Narejñii-Sudarev Method (NSM)

This method divides the flame tube in several film cooling sections. For each section, we calculate the wall's temperature at several points. If the temperatures are under the accepted maximum on the entire length of the section, the geometry chosen is correct. If not, the cooling of the section must be improved by intensifying the heat exchange between the metal

and the film cooling or the section length must be reduced (the length of the section represents the distance between two rows of air inlets).

It is considered that the section is cooled only by its own air film. It is possible to assume that the air film left by the previous section continues to exist, but his temperature is almost equal to that of the hot gases and thus it does not participate to the cooling process any more.

NSM approximates that the temperature is the same on the both faces of the flame tube and, as a result, the term K_{12} and the equation in which it is involved disappears from the equation system (1).

2.1.1. *The heat flow R_1* is obtained by calculating the effective temperature T_f of the flame and the total emissivity of the flame.

First we adopt $T_f = T_{\text{teor}}$, where T_{teor} is the theoretical temperature of the burning gases at the end of the initial burning zone. Assuming that the flame is a grey body

$$(2) \quad R_1 = \sigma_0 \varepsilon_{tf} \varepsilon_f (T_f^4 - T_{tf}^4),$$

where σ_0 is the Stefan-Boltzmann's constant, ε_{tf} is the emissivity of the flame tube's wall and T_{tf} is the temperature of the flame tube's wall.

The values ε_{tf} and T_{tf} are interdependent and are obtained by iteration, as shown in Appendix A.

2.1.2. *The heat flow R_2* is calculated with

$$(3) \quad R_2 = \sigma_0 \varepsilon_{tf} \varepsilon_{ie} (T_{tf}^4 - T_{ie}^4),$$

where ε_{ie} is the emissivity of the outer cover of the combustion chamber, T_{ie} is the temperature of the outer cover of the combustion chamber; it is considered that $T_{ie} = T_a + (20...80)\text{K}$.

2.1.3. *The heat flow C_1* is calculated considering that the cooling air film is modeled by a semilimited jet. It is considered that the jet is formed by an initial zone (in which there are points where the velocity is equal to w_0 at the air inlet) and by a main zone (where the velocity is less than w_0). The heat exchange is analyzed in a different way on the two sections of the jet.

On the initial zone of the jet the following relation can be written

$$(4) \quad C_{1in} = 0.0255 \left(w_0 \frac{x}{v_a} \right)^{0.8} \frac{\lambda_a}{x} (T_{tf} - T_0),$$

where w_0 is the initial velocity of the semilimited jet, x – the distance between the jet's entrance and the current section; λ_a is the thermal conductivity of the air, ν_a – the kinematic viscosity of the air and T_0 is the initial temperature of the semilimited jet.

On the main zone comes true the relation

$$(5) \quad C_{1b} = 0.038 \left(w_{\max} \frac{x}{v_a} \right)^{0.8} \frac{\lambda_a}{x} (T_{tf} - T_{ax}),$$

where w_{\max} is the maximum velocity in the main zone of the jet and T_{ax} is the air temperature on the jet axis (the axis is geometrical position of the points in which the velocity is maximum).

The temperature on the jet axis is determined using the thermal balance equation written for an elementary volume of the jet. The relation is found in Appendix A.

2.1.4. *The heat flow C_2 is calculated with the relation*

$$(6) \quad C_2 = 0.0319 \left(\frac{w_{ci} l_t}{v_a} \right)^{0.8} \frac{\lambda_a}{l_t} (T_{tf} - T_a),$$

where w_{ci} is the air velocity in the annular cavity. For the combustion chambers of the gas turbines the annular cavity width b_{ci} is so chosen that the boundary layer (having δ_2 as width) that appears on the outer surface of the flame tube and the boundary layer (having δ_{ie} as width) that appears on the outer cover are not able to get in touch.

Due to the amount of heat received from the outer surface of the flame tube, the cooling air of a certain section will be warmer than the one of the previous section.

2.2. Lefebvre Method (LM)

2.2.1. *The transversal conduction heat flow through the flame tube's wall K_{12} is determined accordingly to the temperature gradient on the wall thickness*

$$(7) \quad K_{12} = \frac{\lambda_{tf}}{s_{tf}} (T_{tf1} - T_{tf2}),$$

where λ_{tf} is the thermal conductivity of the flame tube's material, s_{tf} is the flame tube's wall thickness and T_{tf1} and T_{tf2} are the temperatures on either the inner and the outer surface of the flame tube's considered section.

2.2.2. The heat flow R_1 is calculated with the relation

$$(8) \quad R_1 = 0.5 (1 + \varepsilon_{tf}) \sigma_0 \varepsilon_f T_f^{1.5} (T_f^{2.5} - T_{f1}^{2.5}),$$

the notations being explained previously.

The calculation method of the emissivity is displayed into Appendix B.

The effective temperature of the flame depends on the heat emission law along the flame tube. That temperature can be determined if known the fuel/air ratio and the combustion efficiency η for the section involved. The most part of the thermic calculations are taken for combustion chamber zones where the combustion efficiency is very close to 100 %. Such supposition does not prove correct in the initial flame zone, where η is usually less than 90 %.

2.2.3. The heat flow R_2 is calculated with the relation

$$(9) \quad R_2 = \frac{\varepsilon_{tf} \varepsilon_{ie} \sigma_0 (T_{tf_2}^4 - T_a^4)}{\varepsilon_{ie} + \varepsilon_{tf} (1 - \varepsilon_{ie}) (A_2/A_{ie})},$$

where ε_{ie} is the emissivity of the outer cover of the combustion chamber, T_a is the secondary air temperature, A_2 is the outer surface area of the flame tube and A_{ie} is the outer cover area.

2.2.4. The heat flow C_1 can be calculated using two computing models distinguished by the air flow nature on the inner side of the flame tube. If the cooling air velocity w_a is less than the burning gases velocity w_g then for the cooling air flow can be used the turbulent boundary layer model. If $w_a > w_g$ the cooling air flow (not too far from the air inlets) corresponds to the semilimited jet model.

The two cases differ after the ratio m of the masic velocities of the air and, respectively, of the gases in the current section

$$(10) \quad m = \frac{(\rho w)_a}{(\rho w)_g}$$

For $0.5 < m < 1.3$ (turbulent boundary layer)

$$(11) \quad C_1 = 0.069 \frac{\lambda_a}{x} R e e_x^{0.7} (T_{ad} - T_{if_1}),$$

where λ_a is the air thermal conductivity, x is the distance between the air inlets and the current section, T_{ad} is the adiabatic wall temperature, $R e_x$ is

the Reynolds number for the air in section x ($\mathcal{R}e_x = \rho_a w_a x / \eta_a$), ρ_a is the air density and η_a is the air dynamic viscosity.

The relations needed to find out the adiabatic wall temperature are given in Appendix B.

If $m \in [1.3..4]$ (semilimited jet), then

$$(12) \quad C_1 = 0.1 \frac{\lambda_a}{x} \mathcal{R}e_x^{0.8} \left(\frac{x}{s} \right)^{-0.36} (T_{ad} - T_{t_{f_1}})$$

and the adiabatic wall temperature is calculated with the relations (B2) and (B4) given in Appendix B.

2.2.5. The heat flow C_2 is calculated in assuming that into the annular cavity between the flame tube and the outer cover the air flow is a turbulent one

$$(13) \quad C_2 = 0.02 \frac{\lambda_a}{d_{ci}^{0.2}} \left(\frac{\dot{m}_{ci}}{A_{ci} \eta_a} \right)^{0.8} (T_{t_{f_2}} - T_a),$$

where d_{ci} is the medium hydraulic diameter of the annular cavity, A_{ci} is the cross section area of the annular cavity and \dot{m}_{ci} is the secondary air mass flow in the current section.

3. Results and Interpretations

The two methods presented above were used for the temperature field calculation along the same section of an individual combustion chamber with air film cooling. The combustion chamber geometry and the chamber working condition were identical when each method was applied. The air cooling mass flow for the section involved was the same, the air film conforming to the semilimited jet model. The temperature fields along the section were represented on the same diagram for both methods.

To be able to compare NSM with LM we must analyze the calculation methods of the heat flows in the combustion chamber.

NSM considers that in a certain section the flame tube temperature is constant along the wall thickness. LM draws distinction between the temperatures $T_{t_{f_1}}$ and $T_{t_{f_2}}$ on the inner and outer surface of the flame tube. For this reason NSM does not employ the transversal conduction heat flow K_{12} and consequently T_f results as solution of a single equation. Using K_{12} heat flow, LM requires the thermal conductivity λ_{t_f} . Both methods neglect the longitudinal conduction heat flow K . NSM is a specialized method.

applicable at individual flame tubes with semilimited jet cooling film. LM is a more general method, which can be used at any kind of film cooling flame tube (with semilimited jet or turbulent boundary layer).

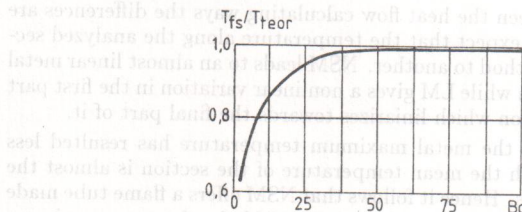


Fig. 2 — The temperature fields.

In which concerns the heat flow R_1 , at NSM the flame tube temperature exponent is 4, while at ML is 2.5. NSM considers only the first reflection of the energy radiated by the two bodies (the flame and the flame tube), while LM uses an experimental dependence that binds the gases absorptivity with the emissivity of the flame tube, which leads to a difference between the two exponents.

To calculate ε_f , NSM uses a radiation attenuating coefficient β determined appealing to empirical relations. Not using the coefficient β , LM employs a complex expression in which appears the luminosity coefficient (an experimental coefficient representing an empirical correction that accommodates the calculations with the experimental data). The mean beam length l_s is calculated likewise, the only difference consisting in the numeric coefficient value (4 at NSM, 3.4 at LM).

The term R_2 is found very similarly. There is a difference in the way of appreciating the outer cover temperature: LM considers that this is equal to the air temperature when entering the combustion chamber while NSM considers it with 20...80° bigger.

The relations used in calculating the heat exchange by convection have similar expressions. NSM uses the relations obtained for the flat plate in forced longitudinal turbulent flow and LM the relations for heat exchange in a straight tube. NSM imposes the calculation of the local values T_{ax} on the thermal boundary layer outer frontier, which implies the solving of a differential equation quite complicate. This problem is solved by LM using the cooling effectiveness, which is determined with a global empiric relation. NSM calculates the air heating in the annular cavity as it goes

along the flame tube, heating which is neglected at LM.

At LM, in the C_2 calculating relation appears explicitly the hydraulic diameter of the annular cavity.

Inasmuch as between the heat flow calculating ways the differences are quite large; it was to expect that the temperature along the analyzed section differs from a method to another. NSM leads to an almost linear metal temperature variation while LM gives a nonlinear variation in the first part of the section, variation which linearizes towards the final part of it.

It was found that the metal maximum temperature has resulted less through LM, although the mean temperature of the section is almost the same at both methods. Hence it follows that NSM offers a flame tube made up from more sections (and shorter, too) than LM, for the same maximum metal temperature.

The temperature calculated with NSM is less than that calculated with LM in the first part of the section, the situation reversing on the final part.

A difficult problem shows up when choosing the physical properties of the gasses at the temperature and especially at the pressures met currently into the gas turbines. In the technical literature are found only incomplete data.

4. Conclusions

The methods shown, even if they differ in the heat flow calculation, lead to similar results. The combustion chamber designed with NSM will use more cooling air than is strictly necessary to maintain the flame tube under the admissible temperature and than a chamber with the same geometry designed with LM.

Appendix A

Auxiliary relations for NSM

Flame emissivity is

$$(A1) \quad \varepsilon_f = 1 - e^{-\beta l_s},$$

where $l_s = 4V/A_i$ is the mean beam length, V is the volume of the flame tube, A_i is the area of the inner surface of the flame tube and $\beta = \beta_g + \beta_p$ is the absorption coefficient for gasses and for particles (especially soot).

The mean absorption coefficient for gasses

$$(A2) \quad \beta_g = \frac{0.8 + 1.6r_{H_2O}}{\sqrt{l_s}} \left(1 - \frac{0.38T_f}{1000} \right) \sqrt{\frac{p}{r_{H_2O} + r_{CO_2}}},$$

where r_{H_2O} and r_{CO_2} are the volumetric participation of H_2O and CO_2 into the burning gases and p is the pressure in the combustion chamber.

For the cross-section j of the combustion chamber

$$(A3) \quad \beta_{g_j} = (0.94 + 0.06l_j)\beta_g,$$

where l_j is the flame relative length — the ratio of the distance between the fuel injector and the cross-section j and the entire length of the flame (between the injector and the mixing zone).

Absorption coefficient of the particles for the diffusive ignition is

$$(A4) \quad \beta_p = \frac{a_f p^{n_f}}{T_f} \left(0.1 + \frac{1.85}{\alpha_1}\right) \left(\frac{1.6T_f}{1000} - 0.5\right) \left(\frac{C}{H}\right)^2,$$

where a_f and n_f are experimental coefficients, $a_f = 2.7 - 2.5(l_j - 0.2)$, $n_f = 1.35 - (0.35/0.8)(l_j - 0.2)$ and C/H is the fuel carbon/hydrogen ratio.

We calculate the mean between the absorption coefficients for n sections

$$\beta_m = \frac{1}{n} \sum_{j=1}^n (\beta_{g_j} + \beta_{p_j}).$$

Using the relation (A1) we calculate the flame mean emissivity for the entire burning zone, $\varepsilon_{f_m} = f(\beta_m)$.

The dependence $T_{f_s}/T_{teor} = f(Bo)$ required to calculate the flame tube temperature is presented in Fig. 3, Boltzmann number being

$$(A5) \quad Bo = \frac{n_s \dot{m} \sum \left(\frac{V}{A_i} (c_p|_{T_a}^{T_{teor}})\right)}{\sigma_0 \varepsilon_{f_m} T_{teor}^3},$$

where n_s is the combustion chamber efficiency, \dot{m}_c is the fuel flow, $c_p|_{T_a}^{T_{teor}}$ is the specific heat at constant pressure (mean on the temperature interval between T_a and T_{teor}) and T_a is the air temperature when entering the combustion chamber.

Effective temperature of the flame in a certain cross-section

$$(A6) \quad T_{f_j} = T_{f_s} \frac{1 - \exp[-0.7/(1 - \sqrt{l_j})]}{1 - (1 - l_j)(T_{teor}^{max} - T_{f_s})/T_{teor}^{max}},$$

T_{teor}^{max} being determined for air excess $\alpha = 1$.

Temperature in jet axis

$$(A7) \quad T_{ax} = \frac{T_m(0.45 + 0.875\delta_1/b - 0.082T_f)}{0.368 + 0.77\delta_1/b},$$

where T_m is the mean temperature on the jet current section (in assuming that the flame temperature varies linearly along the combustion chamber), δ_i is the inner flame tube formed boundary layer thickness and b is the semilimited jet outer boundary layer thickness.

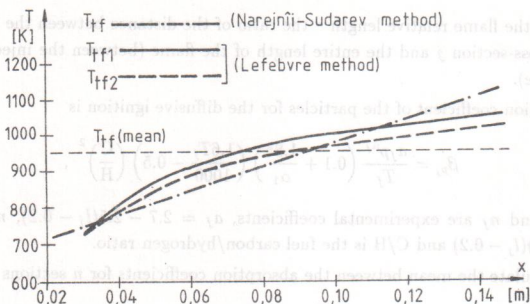


Fig. 3 — Flame temperature dependence of the Boltzmann number at the end of the fire zone for combustion chambers with telescopic flame tube.

Appendix B

Auxiliary relations for LM

Flame emissivity

$$(B1) \quad \epsilon_f = 1 - \exp\left(-290pL\sqrt{\chi l_s} T_f^{1.5}\right),$$

where L is the luminosity coefficient ($L = 1.7$ for kerosene like fuel), p is the pressure in the combustion chamber, χ is the fuel/air mass ratio; $l_s = 3.4V/A_i$ is the mean beam length, where V is the flame tube volume and A_i is the inner surface area of the flame tube.

Cooling effectiveness

$$(B2) \quad \eta = \frac{T_f - T_{ad}}{T_f - T_a},$$

for turbulent boundary layer being

$$(B3) \quad \eta = 0.6 \left(\frac{x}{ms}\right)^{-0.3} \left(\frac{\Re_{es} \eta_a}{\eta_g}\right)^{0.15},$$

where s is the height of the gap through which flows the air film and η_g is the dynamic viscosity for burning gases.

From the above two relations we calculate the adiabatic wall temperature.

The conditions in which the relation (B3) can be applied are

$$0.8 \leq \frac{\rho_a}{\rho_g} \leq 2.5, \quad 0.19 \text{ cm} \leq s \leq 0.64, \quad 0 \leq \frac{x}{s} \leq 150, \quad 0.5 \leq m \leq 1.3.$$

The relation (B3) describes with an error of $\pm 5\%$ the experimental data obtained by [1].

Cooling effectiveness for a semilimited jet is given by

$$\eta = 3.4 \sqrt{\frac{x}{s} \left(1 - \frac{w_g}{w_a}\right)}.$$

Received November 25, 1998

Technical University "Gh. Asachi", Jassy.
Department of Thermal Engines

REFERENCES

1. L e f e b r A., *Profesi v kamerah sgorania TGD*. Izd. Mir, Moskva, 1986.
2. N a r e j n i i E. G., S u d a r e v A. V., *Kameri sgorani v sudovich gazoturbinnih ustanovok*. Sudostroenie, Leningrad, 1973.
3. M a n o l e I., *Construcția și calculul turbomotoarelor de aviație*. Vol. II, București, 1976.

ANALIZĂ COMPARATIVĂ A METODELOR ACTUALE DE DETERMINARE A TEMPERATURII TUBULUI DE FOC CU RĂCIRE PELICULARĂ FOLOSIT LA MOTOARELE CU TURBINĂ CU GAZE

(Rezumat)

Se analizează comparativ metodele N a r e j n i i - S u d a r e v și L e f e b v r e de determinare prin calcul a câmpului de temperatură în lungul unui tronson al tubului de foc răcit pelicular. Pentru condiții identice sunt prezentate câmpurile de temperatură calculate cu cele două metode.